

# Mimicking Melanosomes: Polydopamine Nanoparticles as Artificial Microparasols

Yuran Huang,<sup>†</sup> Yiwen Li,<sup>‡,§</sup> Ziyang Hu,<sup>†</sup> Xiujun Yue,<sup>||</sup> Maria T. Proetto,<sup>‡</sup> Ying Jones,<sup>⊥</sup> and Nathan C. Gianneschi<sup>\*,†,‡,§</sup>

<sup>†</sup>Materials Science and Engineering Program, University of California San Diego, 9500 Gilman Drive, La Jolla, California 92037, United States

<sup>‡</sup>Department of Chemistry and Biochemistry, University of California San Diego, 9500 Gilman Drive, La Jolla, California 92037, United States

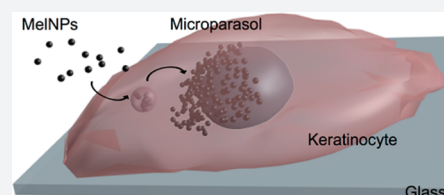
<sup>§</sup>College of Polymer Science and Engineering, State Key Laboratory of Polymer Materials Engineering, Sichuan University, Chengdu 610065, China

<sup>||</sup>Department of Nanoengineering, University of California San Diego, 9500 Gilman Drive, La Jolla, California 92037, United States

<sup>⊥</sup>Electron Microscopy Core Facility, University of California San Diego, 9500 Gilman Drive, La Jolla, California 92037, United States

## S Supporting Information

**ABSTRACT:** A primary role of melanin in skin is the prevention of UV-induced nuclear DNA damage to human skin cells, where it serves to screen out harmful UV radiation. Melanin is delivered to keratinocytes in the skin after being excreted as melanosomes from melanocytes. Defects in melanin production in humans can cause diseases, many of which currently lack effective treatments due to their genetic origins (e.g., skin cancer, vitiligo, and albinism). The widespread prevalence of melanin-related diseases and an increasing interest in the performance of various polymeric materials related to melanin necessitates novel synthetic routes for preparing melanin-like materials. In this work, we prepared melanin-like nanoparticles (MelNPs) via spontaneous oxidation of dopamine, as biocompatible, synthetic analogues of naturally occurring melanosomes, and investigated their uptake, transport, distribution, and UV-protective capabilities in human keratinocytes. Critically, we demonstrate that MelNPs are endocytosed, undergo perinuclear aggregation, and form a supranuclear cap, or so-called microparasol in human epidermal keratinocytes (HEKa), mimicking the behavior of natural melanosomes in terms of cellular distribution and the fact that they serve to protect the cells from UV damage.



Natural melanins are found across animal and plant kingdoms, where they perform various biological functions, including photoprotection, photosensitization, free radical quenching, metal ion chelation,<sup>1</sup> and neuroprotection in the central nervous system of humans.<sup>2,3</sup> Several types of melanins exist in the human body, including eumelanin,<sup>4</sup> pheomelanin,<sup>5</sup> and neuromelanin.<sup>6</sup> Eumelanin is the most common, primarily determining the color of human skin. More importantly, it prevents UV-induced nuclear DNA damage of human skin cells by screening out harmful UV radiation.<sup>7</sup> Solar UV radiation is absorbed by DNA and damages nuclei in epidermal cells, which can lead to the formation of mutations and subsequent, irrecoverable damage. Notably, most natural melanins are mixtures of eumelanins and pheomelanin with various ratios. Pheomelanin shows phototoxicity when complexed with Fe<sup>3+</sup> by stimulating UV-induced lipid peroxidation.<sup>8,9</sup> Therefore, pure, synthetic alternatives may provide a desirable route to repigmentation.

In the basal layer of the epidermis, specialized melanocytes produce melanin-containing organelles, termed melanosomes, in which melanin is synthesized and deposited.<sup>10</sup> In skin, melanosomes are transferred from melanocytes to neighboring

keratinocytes to form perinuclear melanin caps.<sup>11,12</sup> The melanosomes accumulate around the nuclei in the form of melanin caps for the mitigation of UV damage to DNA. Indeed, people are generally familiar with the process by which exposure to UV-radiation causes melanogenesis, observed as a change in skin color commonly referred to as tanning.<sup>13</sup> The integrated biological system for the induction, production, transfer, and degradation of melanosomes is significant for the health of human skin, with melanin-defective diseases, such as vitiligo and albinism, highlighting the importance of these processes. For example, vitiligo develops when the immune system wrongly attempts to clear normal melanocytes from the skin, effectively stopping the production of melanosomes.<sup>14,15</sup> Albinism is caused by genetic defects causing the failure of a copper-containing tyrosinase involved in the production of melanin.<sup>16,17</sup> Both diseases lack effective treatments, and they both promote significant risk of skin cancer in patients.

Water-dispersible, melanin-like polydopamine nanoparticles (MelNPs) with high biocompatibility have been investigated

Received: August 16, 2016

Published: May 18, 2017

for various biomedical applications, including as iron-chelated  $T_1$ -weighted MRI contrast agents,<sup>18</sup> and in targeted therapeutic and bioresponsive applications.<sup>19</sup> MelNPs are prepared synthetically via the spontaneous oxidative polymerization of dopamine under alkaline conditions in aqueous solution.<sup>20</sup> By contrast, biosynthetic melanins are formed in epidermal melanocytes involving tyrosinase-catalyzed oxidative polymerization of tyrosine,<sup>21</sup> giving rise to black, insoluble eumelanins.<sup>22</sup> Both synthetic and biosynthetic melanins appear to consist of largely planar oligomeric scaffolds.<sup>23</sup> MelNPs can be prepared in a variety of sizes and shapes, including spheres,<sup>18</sup> nanorods,<sup>24</sup> and hollow spheres.<sup>25,26</sup> These various morphologies are prevalent in nature, such as in bird feathers, where they play a shape- and packing-dependent role as iridescent structural color elements.<sup>27</sup> However, extraction of melanins from natural sources can be problematic and potentially more complex than direct synthetic routes. Therefore, synthetic MelNPs have been used as models for exploring the function and mechanism of natural eumelanins. For example, our own work on MelNPs has shown that synthetic forms can be used to mimic the performance of bird feathers in terms of structural coloration, and the materials themselves can be prepared in a facile and precisely controllable manner.<sup>28</sup>

We hypothesized that synthetic MelNPs would mimic naturally occurring melanosomes and be taken up by keratinocytes and transported intracellularly, providing photoprotection by adopting the same kind of perinuclear melanin cap in human epidermal keratinocytes as is observed for natural melanin. This hypothesis was predicated on two known facts. First, the process of transfer of melanosomes from melanocytes to keratinocytes can occur when these two cell types are cocultured *in vitro*.<sup>10,29</sup> Second, synthetic fluorescent microspheres had been used to establish the role of the dynactin p150Glued subunit as a required part of the cellular machinery for keratinocytes in which the knockout showed a lack of microparasol formation.<sup>30</sup> To test our hypothesis, we first synthesized spherical MelNPs by spontaneous oxidation of dopamine under alkaline conditions, introducing aqueous ammonium hydroxide to an aqueous solution of monomers (Figure 1).<sup>31</sup> The resulting spherical MelNPs showed a narrow size distribution around 200 nm, observed by transmission electron microscopy (TEM) (Figure 1a), scanning electron microscopy (SEM) (Figure 1b) and dynamic light scattering (DLS) (Figure S1). Energy dispersive X-ray (EDX) measurements demonstrated that the elemental composition (C, N, O) of MelNPs is consistent with natural eumelanin (Figure S2).<sup>32,33</sup> Additionally, Fourier transform infrared spectroscopy (FTIR) of MelNPs showed signals consistent with natural eumelanin including carboxylic acids ( $1038\text{ cm}^{-1}$ ), hydroxyls ( $3225\text{ cm}^{-1}$ ),  $\text{-C=O}$  ( $1617\text{ cm}^{-1}$ ),  $\text{-C=C-}$  bond ( $2156\text{ cm}^{-1}$ ), and  $\text{-C-N=}$  bond ( $1402\text{ cm}^{-1}$ ) (Figure S3).<sup>34</sup> Eumelanin in the condensed phase and in solution has a well-known, broad-band monotonic absorbance, including in the ultraviolet and the visible range.<sup>35</sup> Aqueous solutions of MelNPs appeared black in color (Figure 1c, inserted photograph) with a broad absorption in the UV-vis spectrum from 250 to 850 nm, consistent with eumelanin extracted from natural organelles.<sup>35</sup> To gain insight into the chemical structure of the particles, the MelNPs were analyzed using MALDI-TOF mass spectrometry. The signals with high intensities revealed oligomeric structures consistent with 5,6-dihydroxyindole (DHI) and 5,6-dihydroxyindole-2-carboxylic acid (DHICA) (Figure S4). Similar monomeric units have been observed

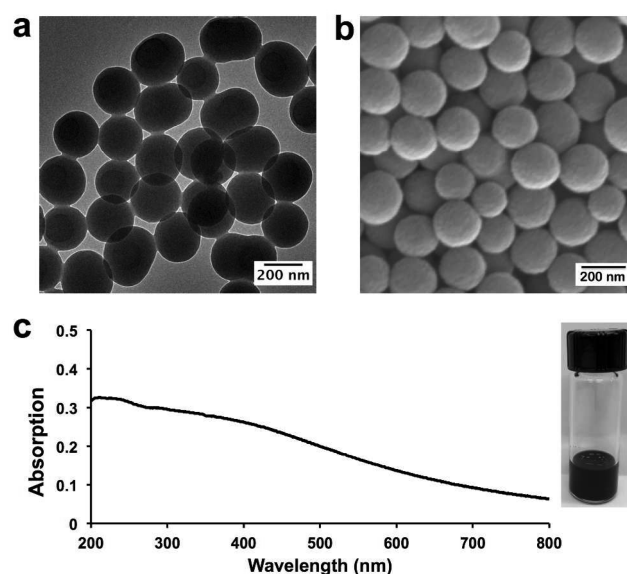


**Figure 1.** Synthesis and characterization of synthetic polydopamine nanoparticles (MelNPs). (a) Unstained TEM image and (b) SEM image of MelNPs. (c) UV-vis spectrum for an aqueous solution of MelNPs and photograph of a vial containing a sample.

previously by MALDI-MS analyses of natural sepia eumelanin.<sup>36,37</sup>

Uptake of synthetic MelNPs into human epidermal keratinocytes (HEKa) was first examined with respect to the concentration dependence (Figure S5) and time dependence of the process (Figure S6). Initially, MelNPs at concentrations of 0.4, 0.1, and 0.02 mg/mL were incubated with HEKa cells for 4 h. TEM images of the cells indicated that MelNPs were taken up. However, some MelNPs tended to adhere to the cell membrane at high concentrations (0.4 and 0.1 mg/mL). Therefore, a concentration of 0.02 mg/mL was chosen for subsequent experiments. In a prior study, Ichihashi et al. extracted natural melanosomes from melanocytes and studied their interactions with keratinocytes. It has been shown that the melanosomes are gradually degraded, leading to the melanin being dispersed around the nucleus of the keratinocytes asymmetrically in a process occurring over the time course of 24 h.<sup>12</sup> Therefore, to test whether MelNPs showed similar behavior, they were incubated at 0.02 mg/mL with HEKa cells and observed at 4 h, 1 day, 2 days, and 3 days (Figure 2). MelNPs were observed as black regions under bright-field confocal microscopy. At 4 h, the confocal images revealed MelNPs (black) surrounding the nuclei (blue), with others distributed in the cytoplasm, which was consistent with TEM data (Figure 2, Figure S6, and Figure S7). However, after 1 day of incubation, melanin accumulated unevenly in the perinuclear area in a manner that appears consistent with observations of natural melanosomes. After 3 days incubation, the MelNPs showed clear signs of morphological transformation (Figure 2, Figure S7 for 2 day data). Further, we observed that transformed MelNPs and spherical MelNPs exist in some HEKa cells simultaneously, which may be caused by sequential order of uptake into cells, or the time course of processing (Figure 2c). To examine whether these processes were inherent to the MelNPs within keratinocytes, we incubated the particles with mesothelial cells (MeT-5A), chosen as a control epithelial cell type distributed within tissues that do not normally take up and process melanosomes.<sup>38</sup> At the same time points, MelNPs

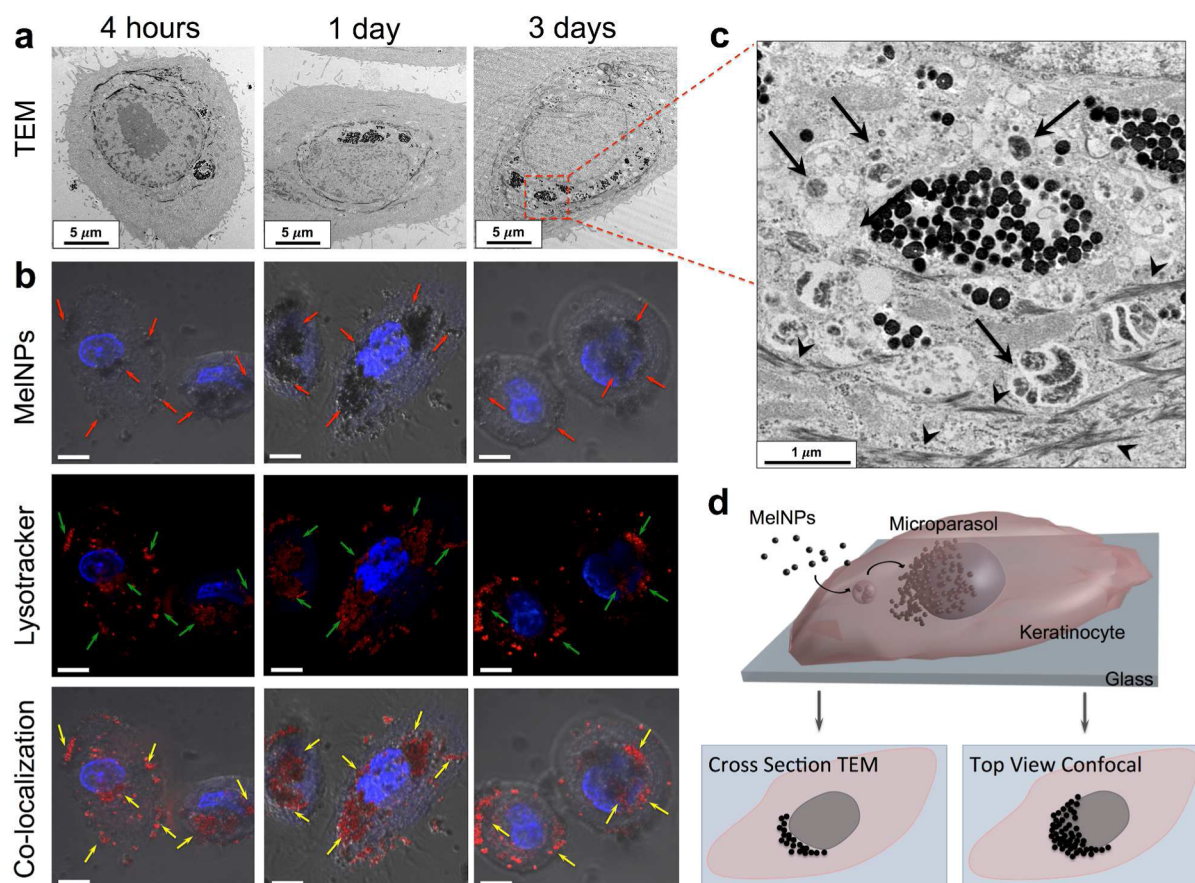


**Figure 2.** Uptake analysis by TEM and confocal light microscopy. (a) TEM images for HEKa cells incubated with 0.02 mg/mL MelNPs for 4 h, 1 day, and 3 days. MelNPs were taken up by HEKa cells and transported to the perinuclear area to form supranuclear caps. For TEM shown here, samples were prepared by flat embedding cells in monolayer cell culture. That is, images are of slices through cells captured as oriented in cell culture, not from pelleted cells. (b) Confocal laser scanning microscopy images for colocalization of MelNPs and lysosomes in HEKa cells. Nuclei of HEKa cells were stained by Hoechst 33342 (blue); lysosomes were stained by LysoTracker Red DND-99 (red, indicated with green arrows); MelNPs were black in HEKa cells under bright field microscopy (indicated with red arrows); the colocalization of bright-field, black MelNPs and red fluorescence for labeled lysosomes are indicated with yellow arrows. Scale bars are 10  $\mu\text{m}$ . (c) Magnification of TEM image for HEKa cells incubated with 0.02 mg/mL MelNPs for 3 days. Melanosomes are indicated with black arrows, and keratin fibers are indicated with black arrowheads. (d) Scheme for the uptake, transportation, and accumulation of MelNPs in HEKa cells and depicted as imaged by the two methods shown here.

lacked any specific trafficking or localization, indicating a random distribution in the cytoplasm (Figure S8). In addition, gold nanoparticles (AuNPs) with a similar size and surface charge to the MelNPs (Figure S9) were incubated with HEKa cells, again showing random dispersion, rather than specific localization (Figure S10). To test for the role of polydopamine surface chemistry on cellular trafficking and distribution in HEKa cells, we prepared two types of core–shell nanoparticles: (1) PDA@SiO<sub>2</sub> nanoparticles consisting of polydopamine cores and SiO<sub>2</sub> shells and (2) SiO<sub>2</sub>@PDA nanoparticles with SiO<sub>2</sub> cores and polydopamine shells. Both core–shell nanoparticles are similar in size and surface charge to MelNPs (Figure S11). Treatment of HEKa cells with SiO<sub>2</sub>@PDA at 0.02 mg/mL resulted in similar accumulation patterns to MelNPs, with particles appearing around the nucleus. By contrast, random accumulation was observed in the case of PDA@SiO<sub>2</sub> nanoparticles (Figure S12 and Figure S13). This suggests that the transport process may be dependent on particle type, and that polydopamine nanoparticle surface chemistry plays a role in governing cellular distribution patterns.<sup>30</sup>

As described in the introduction, melanosomes are tissue-specific, lysosome-related organelles of pigment cells in which melanins are synthesized and stored.<sup>39,40</sup> In epidermal

melanocytes, melanosomes are ultimately transported to neighboring keratinocytes, which retain the melanin while in the basal layer and degrade as they move to the skin surface and differentiate.<sup>41</sup> The melanosome is characterized as a lysosome-related organelle because melanin must be synthesized and polymerized with the help of enzymes and structural proteins within the organelle, where acidic pH seems to be required.<sup>42,43</sup> We hypothesized that the transportation and degradation of MelNPs were similarly driven by a lysosomal process in HEKa cells. To test this hypothesis, we investigated the possible colocalization of lysosomes and MelNPs. We incubated MelNPs with HEKa cells for 4 h, 1 day, and 3 days and stained for lysosomes (LysoTracker, Red DND-99, red, Figure 2). Confocal fluorescence microscopy images show the colocalization of lysosome and melanin (Figure 2b). Therefore, MelNPs might utilize a similar pathway to natural melanosomes, undergoing lysosome-induced degradation and subsequent accumulation to form an artificial perinuclear cap (evident in Figure 2d). After 4 h of incubation, MelNPs appear as clusters in the cytosol surrounded by a membrane (Figure 2a). After 3 days, MelNPs in cells were observed by TEM, without a surrounding membrane in the cytosol and dispersed among keratin fibers (Figure 2c). Similar phenomena were

observed when treating keratinocytes with extracted natural melanosomes,<sup>12</sup> supporting our conclusion that the MelNPs perform as artificial melanosomes utilizing the same transportation and degradation pathway as natural melanosomes.<sup>44,45</sup>

To investigate the photoprotection capability of MelNP perinuclear caps, HEKa cells, after 3 days of incubation with the particles, were treated for 5 min with UV light and subsequently cultured under normal conditions for 1 day. Plain HEKa cells and those incubated with SiO<sub>2</sub>@PDA core-shell nanoparticles, PDA@SiO<sub>2</sub> core-shell nanoparticles, and AuNPs showed dramatically decreased viabilities after UV irradiation. However, HEKa cells incubated with MelNPs displayed significantly higher viability than other groups, at 50%. That is, UV is still detrimental to the cells, but to a decreased level in the presence of MelNPs (Figure 3).

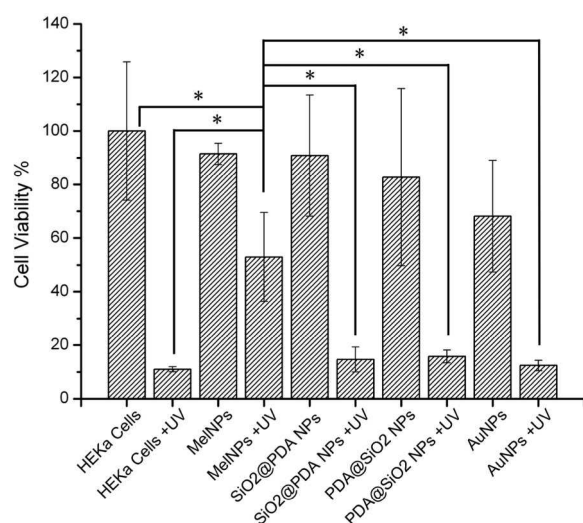


**Figure 3.** HEKa cell viability with and without UV following a 3 day incubation with MelNPs, SiO<sub>2</sub>@PDA core-shell nanoparticles, PDA@SiO<sub>2</sub> core-shell nanoparticles, and AuNPs. \**p* < 0.05.

Furthermore, considering the fact that UV exposure leads to the generation of reactive oxygen species (ROS), resulting in cell death,<sup>46,47</sup> we next assayed for ROS occurring in response to UV irradiation, in the presence of the various nanoparticles described above. Here, we used 2',7'-dichlorofluorescein diacetate (DCFH-DA) as a marker, which exhibits green fluorescence under ROS activation.<sup>48</sup> Following UV irradiation,

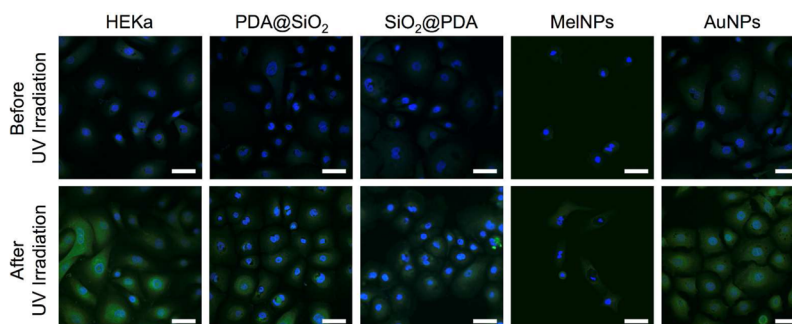


**Figure 4.** Confocal imaging of ROS detection in HEKa cells with MelNPs, SiO<sub>2</sub>@PDA core-shell nanoparticles, PDA@SiO<sub>2</sub> core-shell nanoparticles, and AuNPs after incubation for 3 days. Data is shown before and after 5 min UV irradiation of these cells. The nuclei were stained with NucBlue (blue); ROS generated in HEKa cells were detected with DCFH-DA (green). Scale bars are 50 μm.

the level of green fluorescence in untreated HEKa cells is clearly higher than with MelNP treatment, confirming the protective qualities provided by artificial perinuclear cap formation. Moreover, HEKa cells incubated with PDA@SiO<sub>2</sub> core-shell nanoparticles and AuNPs respectively displayed significant increases in ROS-related green fluorescence. In turn, cells incubated with SiO<sub>2</sub>@PDA core-shell nanoparticles showed low levels of green fluorescence similar to MelNPs, an effect potentially due to their surface exposed polydopamine. Controls without UV irradiation, with all types of nanoparticles, showed low to undetectable levels of green fluorescence (Figure 4, Figure S14). These data imply that ROS can be decreased utilizing particles that deposit polydopamine intracellularly. However, viability assays indicate that only MelNPs provide actual protection. Therefore, we endeavored to examine DNA damage directly.

DNA damage is the predominant deleterious effect of UV radiation on cells. UV radiation induces two of the most abundant mutagenic and cytotoxic DNA lesions known: cyclobutane-pyrimidine dimers (CPDs) and 6-4 photoproducts (6-4PPs) and their Dewar valence isomers.<sup>7,49,50</sup> Therefore, we tested for protective qualities of MelNPs by analyzing DNA damage in HEKa cells after treatment with MelNPs followed by UV irradiation (Figure 5). In mammalian cells, damage to genomic DNA can be lethal, inducing the formation of phosphorylated H2AX.<sup>51</sup> In our study, DNA damage was detected using a red fluorescent antibody (Alexa Fluor 555) against phosphorylated H2AX. At the same time, cell viability was investigated by Image-iT DEAD Green, which permeates when the plasma membrane is compromised. The results show that HEKa cells suffering this treatment had dramatically increased DNA damage (red) and cell death (green), seen simultaneously (see magnified images in Figure S15). By contrast, after incubating with MelNPs for 3 days, HEKa cells with 5 min UV irradiation and subsequent 24 h incubation displayed less DNA damage (Figure 5). In addition, we confirmed that there was no heat generation in MelNPs solutions after UV irradiation (Figure S16). Therefore, the supranuclear artificial melanin caps reduce damage from ultraviolet light in HEKa cells, similar to the performance of natural supranuclear melanin caps.<sup>52</sup>

In conclusion, we prepared melanin-like nanoparticles (MelNPs) by spontaneous oxidation of dopamine in alkaline solution to investigate their potential as mimics of melanosomes. MelNPs were taken up by HEKa cells, followed by accumulation in patterns typical of so-called microparasols or perinuclear caps. This cellular distribution pattern is similar to

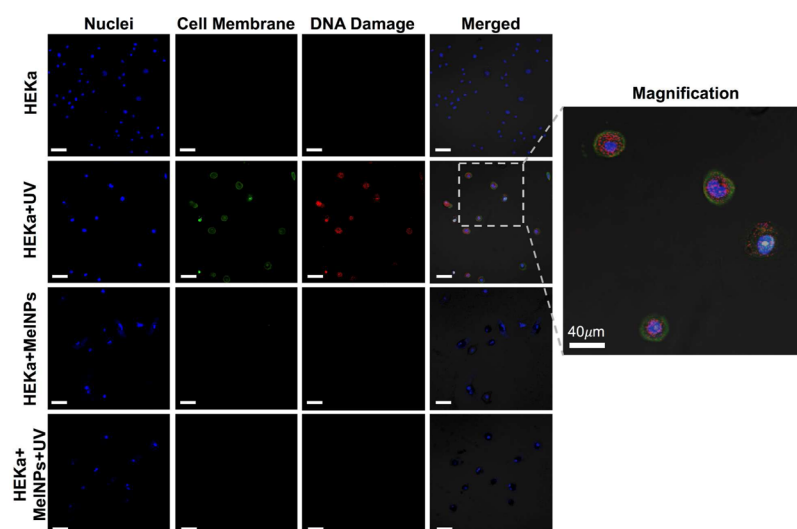


**Figure 5.** Evaluation of MelNPs as protective materials against UV damage to keratinocytes. DNA damage evaluated by light microscopy for HEKa cells with/without incubation with MelNPs. Nuclei were stained by Hoechst 33342 and indicated as blue; cell membranes were stained by Image-iT DEAD Green and shown as green. Scale bars are 80  $\mu\text{m}$ .

that observed for natural melanosomes occurring in human skin in vivo<sup>12</sup> observed in tissue culture of keratinocytes treated with extracted melanosomes,<sup>39</sup> and in cocultures of melanocytes with keratinocytes.<sup>29</sup> We demonstrated the UV photoprotective qualities of synthetic MelNPs, as predominantly arising from the prevention of DNA damage. Considering limitations in the treatment of melanin-defective related diseases and the biocompatibility of these synthetic MelNPs in terms of uptake and degradation, these systems have potential as artificial melanosomes for the development of novel therapies, possibly supplementing the biological functions of natural melanins.

## ■ ASSOCIATED CONTENT

### Supporting Information

The Supporting Information is available free of charge on the ACS Publications website at DOI: [10.1021/acscentsci.6b00230](https://doi.org/10.1021/acscentsci.6b00230).

Synthetic methods, materials characterization, and nanoparticles analysis in cells (PDF)

## ■ AUTHOR INFORMATION

### Corresponding Author

\*E-mail: [ngianneschi@ucsd.edu](mailto:ngianneschi@ucsd.edu).

### ORCID

Yiwen Li: [0000-0002-6874-0350](https://orcid.org/0000-0002-6874-0350)

Nathan C. Gianneschi: [0000-0001-9945-5475](https://orcid.org/0000-0001-9945-5475)

### Notes

The authors declare no competing financial interest.

## ■ ACKNOWLEDGMENTS

The authors acknowledge the generous support of the Department of Defense, Air Force Office of Scientific Research (AFOSR) for a PECASE Award to N.C.G. (FA9550-11-1-0105).

## ■ REFERENCES

(1) Hong, L.; Simon, J. D. Current understanding of the binding sites, capacity, affinity, and biological significance of metals in melanin. *J. Phys. Chem. B* **2007**, *111*, 7938–7947.

(2) Ju, K.-Y.; Lee, J. W.; Im, G. H.; Lee, S.; Pyo, J.; Park, S. B.; Lee, J. H.; Lee, J.-K. Bio-Inspired, Melanin-Like Nanoparticles as a Highly Efficient Contrast Agent for T1-Weighted Magnetic Resonance Imaging. *Biomacromolecules* **2013**, *14*, 3491–3497.

(3) d'Ischia, M.; Wakamatsu, K.; Cicoira, F.; Di Mauro, E.; Garcia Borrón, J. C.; Commo, S.; Galván, I.; Ghanem, G.; Kenzo, K.; Meredith, P. Melanins and melanogenesis: from pigment cells to human health and technological applications. *Pigm. Cell Melanoma Res.* **2015**, *28*, 520–544.

(4) Hunt, G.; Kyne, S.; Ito, S.; Wakamatsu, K.; Todd, C.; Thody, A. J. Eumelanin and pheomelanin contents of human epidermis and cultured melanocytes. *Pigm. Cell Res.* **1995**, *8*, 202–208.

(5) Ito, S.; Wakamatsu, K. Quantitative analysis of eumelanin and pheomelanin in humans, mice, and other animals: a comparative review. *Pigm. Cell Res.* **2003**, *16*, 523–531.

(6) Zucca, F. A.; Basso, E.; Cupaioli, F. A.; Ferrari, E.; Sulzer, D.; Casella, L.; Zecca, L. Neuromelanin of the human substantia nigra: an update. *Neurotoxic. Res.* **2014**, *25*, 13–23.

(7) Brenner, M.; Hearing, V. J. The Protective Role of Melanin Against UV Damage in Human Skin. *Photochem. Photobiol.* **2008**, *84*, 539–549.

(8) Ito, S.; Wakamatsu, K. Chemistry of mixed melanogenesis—pivotal roles of dopaquinone. *Photochem. Photobiol.* **2008**, *84*, 582–592.

(9) Simon, J. D.; Peles, D. N. The red and the black. *Acc. Chem. Res.* **2010**, *43*, 1452–1460.

(10) Taiëb, A.; Cario-André, M.; Briganti, S.; Picardo, M.; Borovansky, J.; Riley, P. Wiley-VCH Verlag GmbH & Co.: Weinheim, 2011.

(11) Wu, X. S.; Masedunskas, A.; Weigert, R.; Copeland, N. G.; Jenkins, N. A.; Hammer, J. A. Melanoregulin regulates a shedding mechanism that drives melanosome transfer from melanocytes to keratinocytes. *Proc. Natl. Acad. Sci. U. S. A.* **2012**, *109*, E2101–E2109.

(12) Ando, H.; Niki, Y.; Ito, M.; Akiyama, K.; Matsui, M. S.; Yarosh, D. B.; Ichihashi, M. Melanosomes are transferred from melanocytes to keratinocytes through the processes of packaging, release, uptake, and dispersion. *J. Invest. Dermatol.* **2012**, *132*, 1222–1229.

(13) Tadokoro, T.; Kobayashi, N.; Zmudzka, B. Z.; Ito, S.; Wakamatsu, K.; Yamaguchi, Y.; Korossy, K. S.; Miller, S. A.; Beer, J. Z.; Hearing, V. J. UV-induced DNA damage and melanin content in human skin differing in racial/ethnic origin. *FASEB J.* **2003**, *17*, 1177–1179.

(14) Jin, Y.; Birlea, S. A.; Fain, P. R.; Ferrara, T. M.; Ben, S.; Riccardi, S. L.; Cole, J. B.; Gowan, K.; Holland, P. J.; Bennett, D. C. Genome-

wide association analyses identify 13 new susceptibility loci for generalized vitiligo. *Nat. Genet.* **2012**, *44*, 676–680.

(15) Alikhan, A.; Felsten, L. M.; Daly, M.; Petronic-Rosic, V. Vitiligo: a comprehensive overview: part I. Introduction, epidemiology, quality of life, diagnosis, differential diagnosis, associations, histopathology, etiology, and work-up. *J. Am. Acad. Dermatol.* **2011**, *65*, 473–491.

(16) Lee, H.; Purohit, R.; Sheth, V.; Papageorgiou, E.; Maconachie, G.; McLean, R. J.; Patel, A.; Pilat, A.; Anwar, S.; Sarvanathan, N. Retinal development in albinism: a prospective study using optical coherence tomography in infants and young children. *Lancet* **2015**, *385*, S14.

(17) Montoliu, L.; Grønskov, K.; Wei, A. H.; Martínez-García, M.; Fernández, A.; Arveiler, B.; Morice-Picard, F.; Riazuddin, S.; Suzuki, T.; Ahmed, Z. M. Increasing the complexity: new genes and new types of albinism. *Pigm. Cell Melanoma Res.* **2014**, *27*, 11–18.

(18) Ju, K. Y.; Lee, S.; Pyo, J.; Choo, J.; Lee, J. K. Bio-inspired Development of a Dual-Mode Nanoprobe for MRI and Raman Imaging. *Small* **2015**, *11*, 84–89.

(19) Liu, Y.; Ai, K.; Lu, L. Polydopamine and its derivative materials: synthesis and promising applications in energy, environmental, and biomedical fields. *Chem. Rev.* **2014**, *114*, 5057–5115.

(20) Ju, K.-Y.; Lee, Y.; Lee, S.; Park, S. B.; Lee, J.-K. Bioinspired polymerization of dopamine to generate melanin-like nanoparticles having an excellent free-radical-scavenging property. *Biomacromolecules* **2011**, *12*, 625–632.

(21) Ando, H.; Kondoh, H.; Ichihashi, M.; Hearing, V. J. Approaches to identify inhibitors of melanin biosynthesis via the quality control of tyrosinase. *J. Invest. Dermatol.* **2007**, *127*, 751–761.

(22) d'Ischia, M.; Napolitano, A.; Pezzella, A. S, 6-Dihydroxyindole Chemistry: Unexplored Opportunities Beyond Eumelanin. *Eur. J. Org. Chem.* **2011**, *2011*, 5501–5516.

(23) Watt, A. A.; Bothma, J. P.; Meredith, P. The supramolecular structure of melanin. *Soft Matter* **2009**, *5*, 3754–3760.

(24) Yu, X.; Fan, H.; Wang, L.; Jin, Z. Formation of polydopamine nanofibers with the aid of folic acid. *Angew. Chem., Int. Ed.* **2014**, *53*, 12600–12604.

(25) Ochs, C. J.; Hong, T.; Such, G. K.; Cui, J.; Postma, A.; Caruso, F. Dopamine-mediated continuous assembly of biodegradable capsules. *Chem. Mater.* **2011**, *23*, 3141–3143.

(26) Chen, X.; Yan, Y.; Müllner, M.; van Koevorden, M. P.; Noi, K. F.; Zhu, W.; Caruso, F. Engineering fluorescent poly (dopamine) capsules. *Langmuir* **2014**, *30*, 2921–2925.

(27) Wogelius, R.; Manning, P.; Barden, H.; Edwards, N.; Webb, S.; Sellers, W.; Taylor, K.; Larson, P.; Dodson, P.; You, H. Trace metals as biomarkers for eumelanin pigment in the fossil record. *Science* **2011**, *333*, 1622–1626.

(28) Xiao, M.; Li, Y.; Allen, M. C.; Deheyn, D. D.; Yue, X.; Zhao, J.; Gianneschi, N. C.; Shawkey, M. D.; Dhinojwala, A. Bio-Inspired Structural Colors Produced via Self-Assembly of Synthetic Melanin Nanoparticles. *ACS Nano* **2015**, *9*, 5454–5460.

(29) Kasraee, B.; Nikolic, D. S.; Salomon, D.; Carraux, P.; Fontao, L.; Piguat, V.; Omrani, G. R.; Sorg, O.; Saurat, J. H. Ebselen is a new skin depigmenting agent that inhibits melanin biosynthesis and melanosomal transfer. *Exp. Dermatol.* **2012**, *21*, 19–24.

(30) Byers, H. R.; Dykstra, S. G.; Boissel, S. J. Requirement of dynactin p150Glued subunit for the functional integrity of the keratinocyte microparasol. *J. Invest. Dermatol.* **2007**, *127*, 1736–1744.

(31) Bernsmann, F.; Ball, V.; Addiego, F.; Ponche, A.; Michel, M.; Gracio, J. J. d. A.; Toniazzo, V.; Ruch, D. Dopamine– melanin film deposition depends on the used oxidant and buffer solution. *Langmuir* **2011**, *27*, 2819–2825.

(32) Ito, S. Reexamination of the structure of eumelanin. *Biochim. Biophys. Acta, Gen. Subj.* **1986**, *883*, 155–161.

(33) Chen, S.-R.; Jiang, B.; Zheng, J.-X.; Xu, G.-Y.; Li, J.-Y.; Yang, N. Isolation and characterization of natural melanin derived from silky fowl (*Gallus gallus domesticus* Brisson). *Food Chem.* **2008**, *111*, 745–760.

(34) Meredith, P.; Sarna, T. The physical and chemical properties of eumelanin. *Pigm. Cell Res.* **2006**, *19*, 572–594.

(35) Tran, M. L.; Powell, B. J.; Meredith, P. Chemical and structural disorder in eumelanins: a possible explanation for broadband absorbance. *Biophys. J.* **2006**, *90*, 743–752.

(36) Strube, O. I.; Büngeler, A.; Bremser, W. Site-Specific In Situ Synthesis of Eumelanin Nanoparticles by an Enzymatic Autodeposition-Like Process. *Biomacromolecules* **2015**, *16*, 1608–1613.

(37) Pezzella, A.; Napolitano, A.; d'Ischia, M.; Prota, G.; Seraglia, R.; Traldi, P. Identification of Partially Degraded Oligomers of 5, 6-Dihydroxyindole-2-carboxylic Acid in Sepia Melanin by Matrix-assisted Laser Desorption/Ionization Mass Spectrometry. *Rapid Commun. Mass Spectrom.* **1997**, *11*, 368–372.

(38) Mutsaers, S. E. The mesothelial cell. *Int. J. Biochem. Cell Biol.* **2004**, *36*, 9–16.

(39) Orlow, S. J. Melanosomes are specialized members of the lysosomal lineage of organelles. *J. Invest. Dermatol.* **1995**, *105*, 3–7.

(40) Dell'Angelica, E. C.; Mullins, C.; Caplan, S.; Bonifacio, J. S. Lysosome-related organelles. *FASEB J.* **2000**, *14*, 1265–1278.

(41) Scott, G.; Leopardi, S.; Printup, S.; Madden, B. C. Filopodia are conduits for melanosome transfer to keratinocytes. *J. Cell Sci.* **2002**, *115*, 1441–1451.

(42) Raposo, G.; Marks, M. S. Melanosomes—dark organelles enlighten endosomal membrane transport. *Nat. Rev. Mol. Cell Biol.* **2007**, *8*, 786–797.

(43) Marks, M. S.; Seabra, M. C. The melanosome: membrane dynamics in black and white. *Nat. Rev. Mol. Cell Biol.* **2001**, *2*, 738–748.

(44) d'Ischia, M.; Napolitano, A.; Michalczuk-Wetula, D.; Plonka, P. Melanin “dust” or “ghost”? *Exp. Dermatol.* **2016**, *25*, 505–506.

(45) Okuda, H.; Yoshino, K.; Wakamatsu, K.; Ito, S.; Sota, T. Degree of polymerization of 5, 6-dihydroxyindole-derived eumelanin from chemical degradation study. *Pigm. Cell Melanoma Res.* **2014**, *27*, 664–667.

(46) Szewczyk, G.; Zadło, A.; Sarna, M.; Ito, S.; Wakamatsu, K.; Sarna, T. Aerobic photoreactivity of synthetic eumelanins and pheomelanins: generation of singlet oxygen and superoxide anion. *Pigm. Cell Melanoma Res.* **2016**, *29*, 669–678.

(47) Ito, S.; Pilat, A.; Gerwat, W.; Skumatz, C.; Ito, M.; Kiyono, A.; Zadło, A.; Nakanishi, Y.; Kolbe, L.; Burke, J. M. Photoaging of human retinal pigment epithelium is accompanied by oxidative modifications of its eumelanin. *Pigm. Cell Melanoma Res.* **2013**, *26*, 357–366.

(48) Han, K.; Lei, Q.; Wang, S. B.; Hu, J. J.; Qiu, W. X.; Zhu, J. Y.; Yin, W. N.; Luo, X.; Zhang, X. Z. Dual-Stage-Light-Guided Tumor Inhibition by Mitochondria-Targeted Photodynamic Therapy. *Adv. Funct. Mater.* **2015**, *25*, 2961–2971.

(49) Mouret, S.; Baudouin, C.; Charveron, M.; Favier, A.; Cadet, J.; Douki, T. Cyclobutane pyrimidine dimers are predominant DNA lesions in whole human skin exposed to UVA radiation. *Proc. Natl. Acad. Sci. U. S. A.* **2006**, *103*, 13765–13770.

(50) Premi, S.; Wallisch, S.; Mano, C. M.; Weiner, A. B.; Bacchiocchi, A.; Wakamatsu, K.; Bechara, E. J.; Halaban, R.; Douki, T.; Brash, D. E. Chemiexcitation of melanin derivatives induces DNA photoproducts long after UV exposure. *Science* **2015**, *347*, 842–847.

(51) Kim, S.; Jun, D. H.; Kim, H. J.; Jeong, K.-C.; Lee, C.-H. Development of a high-content screening method for chemicals modulating DNA damage response. *J. Biomol. Screening* **2011**, *16*, 259–265.

(52) Kobayashi, N.; Nakagawa, A.; Muramatsu, T.; Yamashina, Y.; Shirai, T.; Hashimoto, M. W.; Ishigaki, Y.; Ohnishi, T.; Mori, T. Supranuclear melanin caps reduce ultraviolet induced DNA photoproducts in human epidermis. *J. Invest. Dermatol.* **1998**, *110*, 806–810.